Comparison of Micromachined FBAR Band Pass Filters with Different Structural Geometry

Jae Y. Park, Heon M. Lee, Hee C. Lee, Kyeong H. Lee, Young J. Ko,
Jin H. Shin*, Sun H. Moon*, and Jong U. Bu

LG Electronics Institute of Technology
*LG Innotek
16 Woomyeon-Dong Seocho-Gu, Seoul 137-724, Korea

Abstract- **In this paper, fully integrated FBARs (Film Bulk Acoustic Wave Resonators) and FBAR band pass filters have been designed, fabricated, and characterized for advanced mobile/wireless communication systems by using silicon bulk micromachining technology. Two different band pass filters are fabricated and compared with 7 bulk acoustic resonators in series and shunt connection. Various structures are also investigated for finding the better geometry of the FBAR BPF. In addition, dependency of the quality of AlN film on Mo bottom electrode is also presented. The developed AlN film has 1.9° of FWHM (full width half maximum) of rocking curve and approximately 70 MPa in tensile stress on top of the Mo electrode layer. The measured effective coupling coefficient, $K^2_{effective}$ is ranged from 6.8 to 7.3. The fabricated resonator has a quality factor of 1530, insertion loss of –0.45 dB, and return loss of –28 dB, respectively. Fabricated two different (Type-A and Type-B) band pass filters have insertion loss of –1.5 dB and –1.578 dB, return loss of –6 dB and –10 dB, stop band notch of –50 dB and –52 dB, bandwidth of 75 MHz and 70 MHz, 18 MHz and 32 MHz in separation between lower stop band notch and left edge of pass band, and chip size of 1.3 mm x 1.5 mm, respectively.**

I. INTRODUCTION

Recently, there are great demands for RF band pass filters with smaller size/volume, lighter weight, and higher performance for advanced mobile /wireless communication systems. However, the current filter technology using lumped LC elements, ceramic resonators [1], and surface acoustic wave (SAW) resonators [2-3] have difficulties in on-chip integration, power handling capability, and temperature compensation [4]. Thus, the FBAR has been considerably attracted for fabricating the RF filters with small size and low volume. Since the FBAR have much more smaller size than dielectric resonator and lumped LC elements, lower insertion loss (IL) and higher power handling capabilities than SAW device, and full integration with other CMOS/RF IC circuitry for realizing a single chip radio or a transceiver.

In this paper, three core issues are addressed for finding the better piezoelectric materials and geometry for FBAR devices and FBAR filters. First, co-relationship of aluminum nitride and Mo electrode is researched for achieving the higher quality of the piezoelectric film. Second, size dependency of FBAR devices is investigated on their performance characteristics such as insertion loss, return loss, and quality factor. Third, various structures are designed and tested for finding the better geometry of FBAR band pass filters.

II. DESIGN AND FABRICATION

Fig.1 shows a schematic drawing of the proposed micromachined FBAR device. As shown in Fig.1, the proposed resonator is comprised of silicon nitride membrane, bottom electrode, piezoelectric material, and top electrode. The performance characteristics of the FBAR device such as resonant frequency, bandwidth (BW), insertion loss, return loss, and quality factor (Q) are highly related with thickness and quality of both the electrodes and the piezoelectric material. In particular, crystallinity of the piezoelectric material is the most important factor to determine its performance characteristics. The lower is the value of FWHM (full width half maximum) of the piezoelectric material, the better is the performance characteristics of the resonator and filter. Thus, the piezoelectric material needs to have highly c-axis oriented columnar structure.

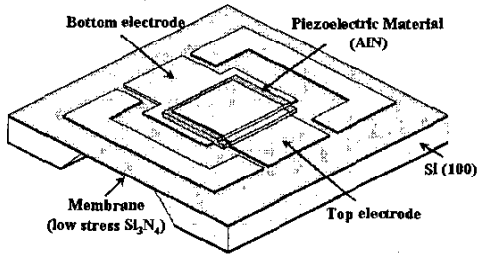

Fig. 1. A schematic drawing of bulk micromachined film bulk acoustic resonator.

0-7803-7695-1/03/$17.00 © 2003 IEEE

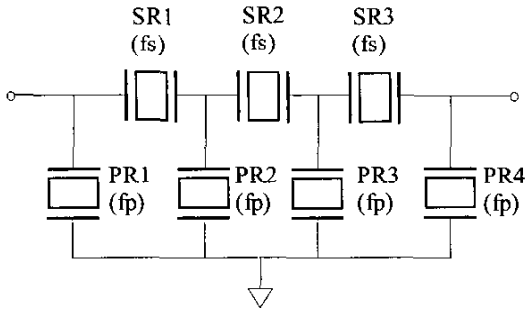

Fig. 2. Topology of the 3.5 stages ladder type FBAR band pass filter.

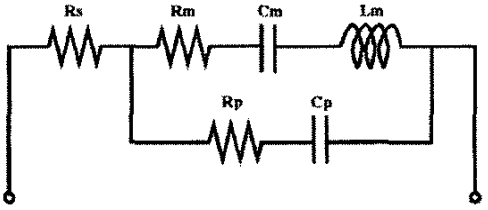

Fig. 3. Modified BVD lumped elements equivalent circuit model of the fabricated film bulk acoustic resonator.

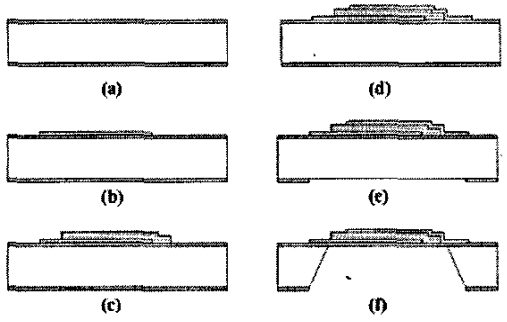

Fig. 4. Fabrication sequences of micromachined FBAR devices and RF band pass filters. (a) silicon nitride deposition, (b) bottom electrode deposition and patterning, (c) piezoelectric layer deposition and patterning, (d) top electrode deposition and patterning, (e) back-side nitride patterning, (f) Si bulk micromachining.

AlN is preferred over ZnO as the piezoelectric material, since it has better silicon compatibility [5], higher phase velocity, higher electrical resistivity, and lower weight density than ZnO. Mo is selected as an electrode material, since it has low acoustic attenuation, low resistivity, large acoustic velocity, and relatively high melting point.

The FBAR device has series (when a polarization is in phase with an applied electrical potential) and parallel resonant (when a polarization is 180 degrees out of phase with an applied electrical potential) frequencies. The difference between the series and parallel resonant frequency is called as a bandwidth of the resonator, and utilized to determine the effective mechanical coupling coefficient, $K^2_{effective}$. It is also important factor to determine the bandwidth of the FBAR filter. The proposed FBAR band pass filters are designed by connecting the resonators in serial and in shunt as shown in Fig. 2. Two stop band notch frequencies of the band pass filter are determined by series resonant frequency of serial resonator, SR1 and parallel resonant frequency of shunt resonator, PR1. Insertion loss is determined by the s_{11} value of PR1 at its series resonant frequency and s_{21} of SR1 at its parallel resonant frequency. Out-of band rejection is determined by the voltage divider ratio between SR1 and PR1 capacitors, since all the FBARs are acting as capacitors in the frequency region far from the pass band. Thus, each size of the serial and shunt FBAR device needs to be optimized for realizing the FBAR band pass filters with lower insertion loss and higher attenuation characteristics. Equivalent circuitry parameters are fitted and extracted for designing the FBAR RF filters by using ADS simulation tool and the modified Butterworth-Van Dyke (MBVD) [6] lumped elements equivalent circuit model shown in Fig. 3.

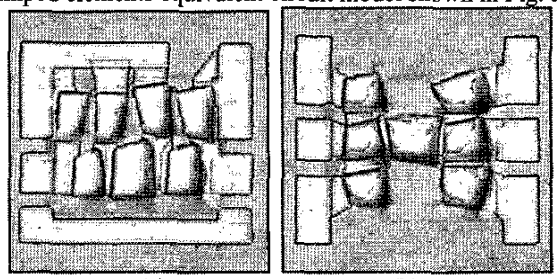

Fig. 5. Photomicrographs of (a) silicon bulk micromachined Type-A and (b) Type-B band pass filters with 7 bulk acoustic resonators.

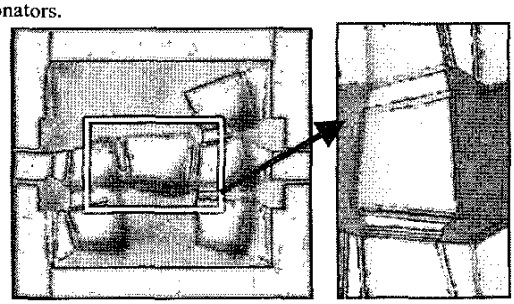

Fig. 6. Photomicrographs of (a) silicon bulk micromachined RF band pass filters with 6 bulk acoustic resonators and (b) a close up view.

The detailed fabrication step of the bulk micromachined FBAR device and FBAR filter is described in Fig. 4. A silicon nitride was deposited on a silicon substrate. Bottom electrode was then deposited and patterned. A piezoelectric layer was sputtered and

patterned on top of the patterned bottom electrode. A top electrode and add layer were deposited and patterned in order. After patterning the silicon nitride at the backside of the silicon substrate, the substrate was etched selectively by using KOH. Fig. 5 shows photomicrographs of the fabricated FBAR RF filters with two different structural geometries (Type-A and Type-B). These two filters are comprised of the same sizes of the resonators, but the locations and shapes of the parallel resonators are different. Fig. 6 shows Type-B filter without a shunt resonator, PR1 and its close up view. As shown in Fig.6, there is no wrinkle on the silicon nitride membrane of the FABR filter.

III. EXPERIMENTAL RESULTS AND DISCUSSIONS

The developed piezoelectric material of AlN and Mo electrode films by using RF magnetron sputtering system were highly preferred to c-axis AlN (002) orientation. As shown in Fig. 7, quality of AlN is strongly dependent on FWHM of the Mo bottom electrode. The aluminum nitride film has 1.9° of FWHM (full width half maximum) of rocking curve and approximately 70 MPa in tensile stress on top of the Mo electrode.

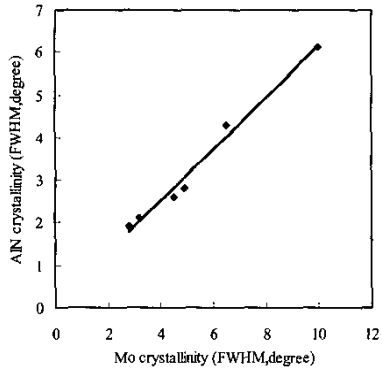

Fig. 7. Measured crystallinity of AlN and Mo films deposited by using RF magnetron sputtering system.

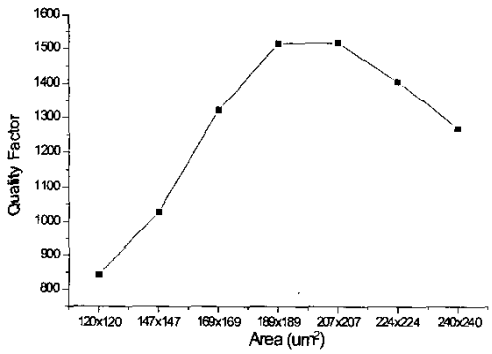

Fig. 8. Dependency of quality factor on the size of the fabricated film bulk acoustic resonator.

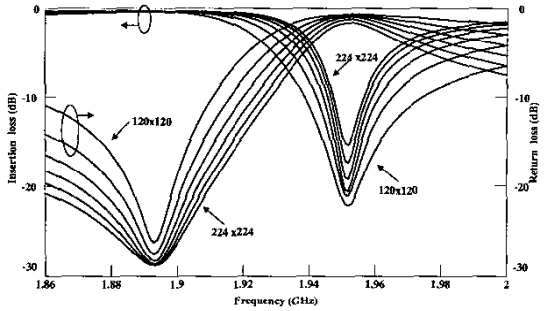

Fig. 9. Dependency of insertion and return losses on the size of the fabricated film bulk acoustic resonator.

Figs. 8 and 9 show the performance characteristics of the fabricated FBAR devices on a silicon nitride supporting membrane. As the size of the resonator is increased, insertion loss, return loss, and quality factor are getting better. But the quality factor starts to degrade over the size of 207 x 207 μm^2.Thus, the size of the resonators should be optimized for designing the filter. The fabricated resonator has the highest quality factor of 1530 with the size ranged from 185 x 185 μm^2 to 207 x 207 μm^2. The Q is dependent on the ohmic resistance in the electrodes, acoustic loss, scattering of the acoustic waves from rough surfaces or grain boundaries, and acoustic radiation into the surrounding area of the devices. The measured effective coupling coefficient, $K^2_{effective}$ is 7.3.

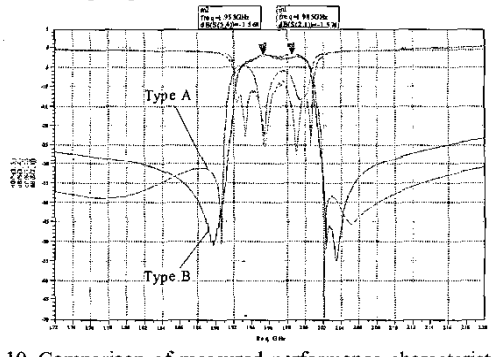

Fig. 10. Comparison of measured performance characteristics of the fabricated Type-A and Type-B FBAR band pass filters.

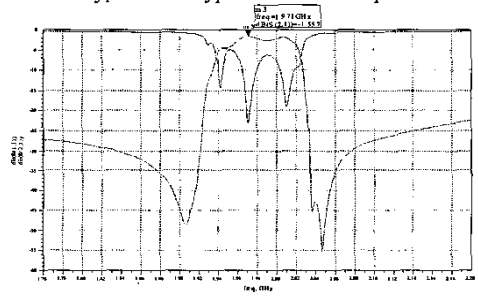

Fig. 11. Measured performance characteristics of the fabricated Type-B BPF with 3 series resonators and 4 shunt resonators.

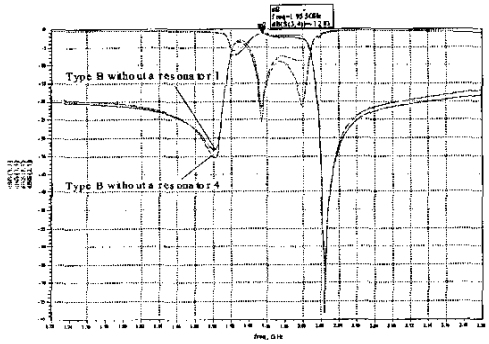

Fig. 12. Comparison of measured performance characteristics of Type-B FBAR band pass filters without the shunt resonator, PR1 or PR4 shown in Fig. 2.

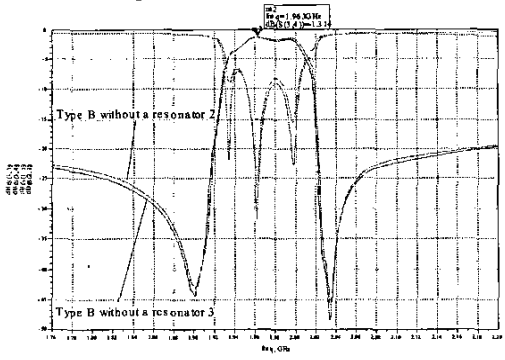

Fig. 13. Comparison of measured performance characteristics of Type-B FBAR band pass filters without the shunt resonator, PR2 or PR3 shown in Fig. 2.

Fig. 10 shows the performance characteristics of the fabricated Type-A and Type-B band pass filters in narrow frequency band. Type-A filter has deeper stop band notches and better sharp skirt and out of band rejection characteristics, while Type-B filter has better return loss characteristics. The different performance characteristics might be caused by the difference of coupling amount of each adjacent resonator and residual stress of the supporting membrane. For evaluating the effect of each shunt resonator on the FBAR band pass filters, the filters with 3 shunt resonators were fabricated, measured, and compared as shown in Fig. 6. Fig. 11 shows the performance characteristics of the fabricated Type-B filters with 3 series resonators and 4 shunt resonators. Figs. 12 and 13 show performance characteristics of the fabricated filters with 3 series resonators and 3 shunt resonators in narrow frequency band. In comparison, the fabricated filters without any input or output shunt resonators (PR1, PR4) have similar performance characteristics. When attenuation at the lower stop band was rapidly degraded, insertion loss was slightly improved compared to the performance characteristics of the original FBAR filter shown in Fig. 11. The fabricated filters without any middle shunt resonators (PR2, PR3) have also similar performance characteristics. While attenuation at the lower stop band was slightly degraded, insertion loss was slightly improved. In other words, the effect of the middle shut resonators on the performance characteristics of the ladder type FBAR filters is less sensitive than the input and output shunt resonators.

IV. CONCLUSION

Integrated FBARs (Film Bulk Acoustic Wave Resonators) and FBAR band pass filters have been newly designed, fabricated, and characterized. RF band pass filters with different structural geometry have been fabricated and compared. The developed AlN piezoelectric film has 1.9° of FWHM (full width half maximum) of rocking curve and approximately 70 Mpa in tensile stress on top of the Mo electrode. The fabricated FBAR has a quality factor of 1530 in size of 200 x 200 μm^2, insertion loss of –0.45 dB, and return loss of –28 dB, respectively. As size of the FBARs is increased, both quality factor and insertion loss are improved but return loss is degraded. The fabricated band pass filters (Type-A and Type-B) have insertion loss of –1.5 dB and –1.578 dB, return loss of –6 dB and –10 dB, stop band notch of –50 dB and –52 dB, 18 MHz and 32 MHz in separation between lower stop band notch and left edge of pass band, and size of 1.3 mm x 1.5 mm, respectively. These proposed FBARs are promising for developing integrated and miniaturized FBAR VCOs, filter banks, dulpexers, RF FEM (Front-End Module), and RF transceiver due to their compatible fabrication sequences with CMOS/RF IC circuitry.

ACKNOWLEDGMENTS

This work was supported by Korea Ministry of Science & Technology under 21st Frontier Intelligent Micro-system Development Project.

REFERENCES

[1] REMEC Wireless. "Ceramic Filters and Duplexers for Base Station and Microcell Applications", *Microwave J ournal*, 39 (10): 170-172, Oct. 1996.

[2] M. Hikita, N. Shibagaki, T. Akagi, and K. Sakiyama, "Design Methodology and Synthesis Techniques for Ladder-type SAW Resonator Coupled Filters", *IEEE Ultrasonics Symposium*, pp. 15-24, 1993

[3] T. Matsuda, et al, "L and S Band Low Loss Filters Using SAW Resonators", *IEEE Ultrasonics Symposium*, pp. 163-167, 1994

[4] R. S. Naik, et al., *IEEE Trans. Utrason., Ferro., and Fr eq. control*, vol. 45, no. 1, pp. 257-263, Jan. 1998.

[5] S. M. Sze, " Physics of Semiconductor Devices", *John Wiley and Sons*, New York, 2nd edition, 1981

[6] J. D. LarsonIII, et al., "A BAW Antenna Diplexer for the 1900 MHz PCS Band", *IEEE Ultrasonics Symposium Digest*, vol. 1, pp. 863-868, 2000